Definition and Computation of Tensegrity Mechanism Workspace

Quentin Boehler[1]
ICube,
University of Strasbourg,
Strasbourg 67000, France
e-mail: quentin.boehler@icube.unistra.fr

Isabelle Charpentier
ICube,
CNRS,
Strasbourg 67000, France
e-mail: icharpentier@unistra.fr

Marc S. Vedrines
ICube,
INSA of Strasbourg,
Strasbourg 67000, France
e-mail: marc.vedrines@insa-strasbourg.fr

Pierre Renaud
ICube,
INSA of Strasbourg,
Strasbourg 67000, France
e-mail: pierre.renaud@insa-strasbourg.fr

Tensegrity mechanisms using linear springs as tensioned elements constitute an interesting class of mechanisms. When considered as manipulators, their workspace remains however to be defined in a generic way. In this article, we introduce a workspace definition and at the same time a computation method, based on the estimation of the workspace boundaries. The method is implemented using a continuation method. As an example, the workspace assessment of a two degrees of freedom (DOF) planar tensegrity mechanism is presented. [DOI: 10.1115/1.4029809]

Keywords: tensegrity mechanism, workspace computation, continuation method

1 Introduction

Following Ref. [1], a tensegrity system can be defined as a system in stable self-equilibrated state comprising a set of compressed components inside a set of tensioned components. In this self-stress state, different levels of prestress can be imposed for a given topology to modify the level of internal forces in the components. A high stiffness-to-mass ratio can thus be reached [2]. In a tensegrity mechanism, some of the components are actuated. Tensegrity mechanisms composed of rigid cables require a complex control. As a consequence, elastic cables or linear springs are usually chosen as tensioned components to ensure equilibrated configurations without tension loss [3–5] so that the mechanism remains in a self-stress state with a given preload. The mechanism represented in Fig. 1 constitutes an example of such tensegrity mechanisms, with two springs used as nonactuated tensioned elements.

Applications range from mobile robots [6] to lightweight robotic arms [7]. When considered as a manipulator, a tensegrity mechanism has a workspace that is first and foremost difficult to define. This is due to the difficulty of analyzing reachable end-effector positions. For a tensegrity mechanism, kinematic constraints associated to the mechanism geometry have to be considered at the same time as self-equilibrium conditions. The so-called form finding methods exist to solve these conditions [8], with for instance potential energy minimization. The determination of a reachable configuration for a tensegrity mechanism remains however more complex than for a rigid-body mechanism. The difficulty comes also from the influence of an external wrench on the mechanism. Due to the self-equilibrium state, the end-effector positions and the internal forces are coupled. Thus, an external wrench modifies the mechanism configuration as well as the internal forces. As a consequence, external wrenches applied to the mechanism must be taken into account in the workspace definition. Up to now, this is not the case to the best of our knowledge. In Refs. [3,9], the authors interestingly define the reachable workspace (RW), but they assume that no external wrench is applied. Its influence is only introduced afterwards by a local analysis [3] to establish a stiffness map. With such a two-step process, the RW of the mechanism cannot be thoroughly evaluated for a given set of wrenches. In this paper, we propose a workspace definition that clarifies this point.

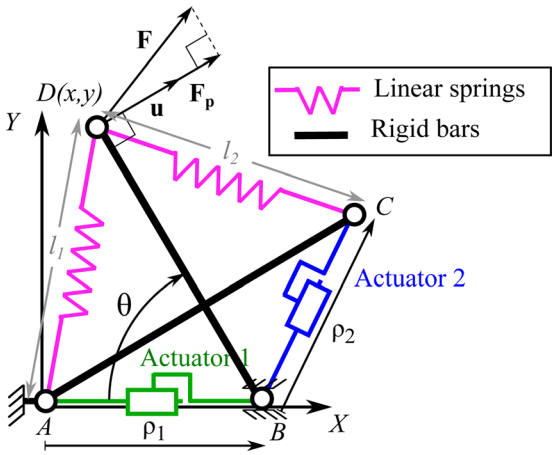

Fig. 1 2DOF planar tensegrity mechanism [3]

Workspace estimation is a first step in the synthesis of a mechanism. In order to integrate usual mechanism requirements, the existence of limits in the actuator ranges and internal forces are to be included as well in the workspace definition. The workspace definition we propose includes such constraints. Exploiting some similarities with the context of cable-driven mechanisms [10], we introduce a workspace definition of interest for tensegrity mechanism design.

Because of the constraints to be handled, workspace computation is also challenging. As a second contribution, this paper introduces a workspace computation strategy. The workspace is obtained by computing all the boundaries introduced by the existing constraints. The interest of the strategy is outlined with an example. Each boundary is assessed with a continuation method [11,12].

In Sec. 2, a definition of the tensegrity mechanism workspace is introduced as well as a computation method. The method is applied on a 2DOF planar mechanism in Sec. 3. Conclusions are finally given on the interest of both the workspace definition and computation.

2 Workspace Definition and Determination

2.1 Workspace Definition. Workspace definition is related to the conditions to be fulfilled at each point in the workspace. These conditions are first summed up. During a robotic task, a given set of external wrenches $\mathbf{W_e}$ is applied on the mechanism

[1]Corresponding author.

Manuscript received July 17, 2014; final manuscript received February 9, 2015; published online April 6, 2015. Assoc. Editor: Pierre M. Larochelle.

end-effector. $\mathbf{W_e}$ is a task-dependent set. A pose belongs to the workspace if it can be reached for any wrench $\mathbf{w_e} \in \mathbf{W_e}$.

Let $\mathbf{q}$ be the generalized coordinates which fully describe the tensegrity mechanism configuration. The set $\mathbf{q}$ is obtained by concatenation of vectors $\mathbf{x}$, $\boldsymbol{\rho}$, and $\boldsymbol{\psi}$ with $\mathbf{x}$ the end-effector pose, $\boldsymbol{\rho}$ the actuated joint coordinates, and $\boldsymbol{\psi}$ complementary coordinates necessary to describe the configuration of each element of the mechanism.

A tensegrity mechanism is in a feasible configuration when it respects the kinematics of the mechanism defined by **kinematic constraints**

$$\boldsymbol{\Phi}(\mathbf{q}) = \mathbf{0} \tag{1}$$

Due to the presence of springs, a subvector $\mathbf{q_u} \subset \mathbf{q}$ cannot be determined by $\boldsymbol{\Phi}$. It is estimated from static conditions, issued from the first derivative of the system potential energy μ [8]

$$\mu = E_{\text{pot}} - V \tag{2}$$

where E_{pot} is the mechanism potential energy, and V the potential function associated to $\mathbf{w_e}$, assumed to be conservative [2]. The **static constraints** describing the tensegrity equilibrium are then expressed as

$$\frac{\partial \mu}{\partial \mathbf{q_u}}(\mathbf{q}, \mathbf{w_e}) = \mathbf{0} \tag{3}$$

In addition, the **configuration stability** is required, which means the Hessian is positive definite [1,2]

$$\frac{\partial^2 \mu}{\partial \mathbf{q_u}^2}(\mathbf{q}, \mathbf{w_e}) > 0 \tag{4}$$

A pose is admissible if and only if the internal forces $\mathbf{t}$ and $\mathbf{f_b}$, respectively, in the springs and the bars are compatible with the sustainable forces in these elements. Similarly, the forces $\mathbf{f_a}$ developed by the actuators are bounded by the components characteristics, as well as the actuator displacements. The following additional set of conditions has therefore to be respected:

$$\boldsymbol{\rho} \in [\boldsymbol{\rho}_{\min}; \boldsymbol{\rho}_{\max}] \tag{5}$$

$$\begin{cases} \mathbf{t} \in [\mathbf{t_{min}}; \mathbf{t_{max}}] \\ \mathbf{f_a} \in [\mathbf{f_{a\,min}}; \mathbf{f_{a\,max}}] \\ \mathbf{f_b} \in [\mathbf{f_{b\,min}}; \mathbf{f_{b\,max}}] \end{cases} \tag{6}$$

where $[\boldsymbol{\rho}_{\min}; \boldsymbol{\rho}_{\max}]$ are the actuation stroke limits, $\mathbf{t_{min}}, \mathbf{f_{a\,min}}$, and $\mathbf{f_{b\,min}}$ are the minimum forces, and $\mathbf{t_{max}}, \mathbf{f_{a\,max}}$, and $\mathbf{f_{b\,max}}$ are the maximum admissible forces in the springs, actuators, and bars, respectively.

Based on the definition of cable-driven robots workspaces [10], we propose to define the set of reachable configurations of a tensegrity mechanism as the wrench feasible workspace (WFW) defined as follows.

DEFINITION 1. *WFW: The WFW of a tensegrity mechanism is defined as the set of all end-effector poses* $\boldsymbol{x}$ *for which a set* $(\boldsymbol{\rho}, \boldsymbol{\psi})$ *exists for all* $\mathbf{w_e} \in \mathbf{W_e}$ *as a solution of the system*

$$\begin{cases} \boldsymbol{\Phi}(\mathbf{q}) = \mathbf{0} \\ \dfrac{\partial \mu}{\partial \mathbf{q_u}}(\mathbf{q}, \mathbf{w_e}) = \mathbf{0} \end{cases} \tag{7,8}$$

and for which the conditions (4)–(6) are fulfilled for any $\mathbf{w_e} \in \mathbf{W_e}$.

In other words, any pose in the WFW must respect the kinematic and the static constraints as well as the set of limits introduced in Eqs. (4)–(6). From the definition of the WFW, it is judicious to also define the RW in the absence of external load, i.e., $\mathbf{W_e} = \{\mathbf{0}\}$. This specific definition may be useful for preliminary mechanism assessment. In the literature, this situation is described as the RW [3].

DEFINITION 2. *RW: The RW of a tensegrity mechanism is defined as the solution of the WFW when* $\mathbf{W_e} = \{\mathbf{0}\}$.

2.2 Workspace Computation. Because of the number and the nature of the conditions that define the WFW, its computation represents a challenge. Indeed, the numerical evaluation of RW, a simplified situation, was only introduced in the literature in a few contexts with the specific case of zero free length springs [3,5]. We propose to determine the WFW by examining its boundaries. The interest of such an approach was demonstrated for rigid manipulators [12], a context for which only kinematic conditions exist.

The workspace computation is therefore performed in the following way. First, the wrench set $\mathbf{W_e}$ is sampled. For a given wrench $\mathbf{w_e} \in \mathbf{W_e}$, the corresponding workspace is computed as detailed below. The WFW is determined as the intersection of the boundaries-enclosed spaces obtained for all the sampled wrenches in $\mathbf{W_e}$.

Since Eqs. (4)–(8) can be considered as a set of limits, each of them is in turn followed to build a workspace limit. In other words, a set of workspace limits is generated by sequentially considering a set of equations containing

(1) **Kinematic constraints** to be fulfilled at every pose in the workspace (Eq. (7)).
(2) **Static constraints** also to be respected (Eq. (8)).
(3) **One limit constraint** that expresses either that:
   — the mechanism is in singularity, i.e., the system (7)–(8) is rank deficient [12]
   — the mechanism is in a stability limit, expressed from Eq. (4)
   — an actuator reaches a stroke limit, derived from Eq. (5)
   — a force limit in a mechanism element is reached, derived from Eq. (6)

The determination of the WFW consists in solving Eqs. (7) and (8) together with, each in turn, one of the limit constraints.

The success of such an approach is based on the ability to obtain the set of poses for which each limit constraint is satisfied and that constitutes a boundary. In the same spirit as Ref. [12], we adopt a continuation method. A first solution along the boundary is obtained using a Newton–Raphson algorithm. Continuous descriptions of the boundaries are then obtained with Taylor approximations [11] using the continuation method. The interested reader is referred to Ref. [13] for an exhaustive description of continuation methods and related software. The strategy used for the workspace computation and its accuracy are illustrated through the example developed in Sec. 3.

3 Workspace Computation of a 2DOF Planar Tensegrity Mechanism

The workspace of the 2DOF planar tensegrity mechanism featured Fig. 1 is assessed. The RW of this mechanism was evaluated in Ref. [3] in the case of zero free length springs. We consider here nonzero free length springs, the general case that can be of interest for the designer, and wish to compute the WFW for sake of comparison.

3.1 Problem Statement. The mechanism is composed of four nodes $\{A, B, C, D\}$. Two rigid bars of length L connect A with C and B with D. Two linear springs of lengths l_1 and l_2 with identical stiffness k and free length l_0 connect, respectively, A with D and C with D forming a preloaded tensegrity. The node A is anchored to the base and B is constrained to move in the

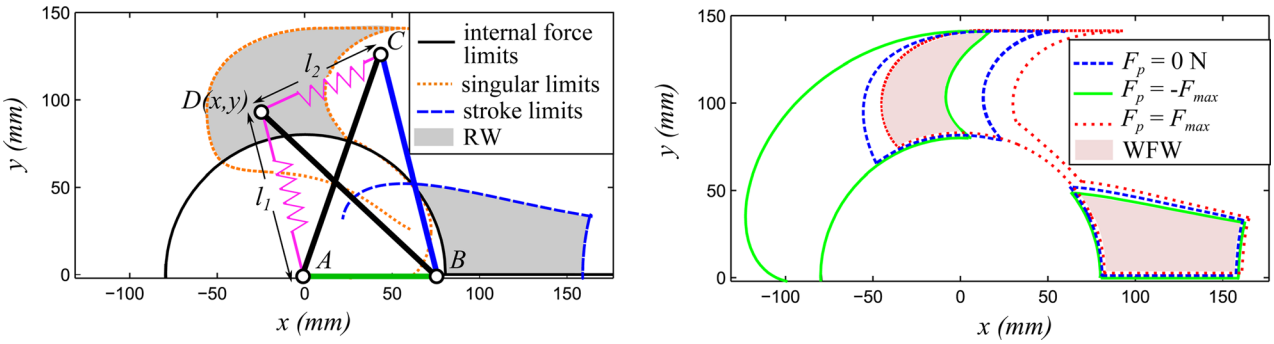

Fig. 2 Computed limits and RW of the mechanism on the left figure. WFW of the mechanism on the right figure. The mechanism configuration for $\rho = (75, 136)$ mm and $F_p = 0$ N is superimposed on the left plot.

X-direction. The actuated joint coordinates are $\boldsymbol{\rho} = (\rho_1, \rho_2)$ and the node D is considered as the end-effector so that $\mathbf{x} = (x, y)$. In the following, $l_0 = 80$ mm, $k = 4$ N/mm, $L = 140$ mm, and we consider as an external wrench a force $\mathbf{F}$ acting on the end-effector. This force is considered to be applied in any possible orientation, with a maximum intensity equal to $F_{\max} = 70$ N.

Actuator strokes are chosen in the range [0; 300] mm for both actuators. In order to ease the interpretation of the results, simple force limits are considered, using only a minimum tension equal to zero in the springs, i.e., no spring compression is admitted. This corresponds to $\mathbf{t_{min}} = \mathbf{0}$.

3.2 Workspace Estimation. The knowledge of $\mathbf{x}$ and $\boldsymbol{\rho}$ allows us to describe the mechanism configuration. No complementary coordinate is needed, and Eq. (7) is here formulated as

$$x - (\rho_1 - \sqrt{L^2 - y^2}) = 0 \tag{9}$$

One can see from Fig. 1 that one mobility is not constrained by the actuators, namely, the rotation of the bar BD around B. Thus, the vector $\mathbf{q_u}$ is here a scalar, that can be arbitrarily chosen as x or y. The mechanism pose can be determined by deriving its potential energy, assumed to be stored in the springs

$$E_{\text{pot}} = \frac{1}{2}k((l_1 - l_0)^2 + (l_2 - l_0)^2) \tag{10}$$

For given values of the actuated joints, a force exerted in the direction of the bar BD cannot modify its position. As a consequence, the potential energy V associated to the external force $\mathbf{F}$ is built by only taking into account the component $\mathbf{F_p}$ that is perpendicular to the bar. We consider $\mathbf{F_p} = F_p\mathbf{u}$, where $\mathbf{u}$ is a unit vector perpendicular to BD as depicted in Fig. 1. The potential energy is then expressed as

$$V = F_p \cdot L \cdot \theta \tag{11}$$

with $\theta = \arccos((\rho_1 - x)/L)$.

The expression of Eq. (8) is obtained by differentiation of Eqs. (10) and (11). A second derivation is performed to get Eq. (4).

In this example, the wrench sampling is simplified by the force limits that have been expressed. A force applied in the direction of the bar BD only modifies the level of force in this bar and in the actuators. No force limit was introduced for these components, thus it is possible to sample F_p in the interval $[-F_{\max}, F_{\max}]$.

Singularities of this mechanism are encountered when the points A, B, and C are aligned. Such a situation does not depend on the spring characteristics, nor on the external force applied on the end-effector. Consequently, the singular limits can be expressed by relationships between the actuated joint coordinates: $\rho_1 \pm \rho_2 = \pm L$, and these limits are considered for the workspace computation.

The evaluation of Eq. (4) shows that no stability limit can be reached. In the workspace computation strategy described in Sec. 2.2, no stability limit constraint is therefore considered.

3.3 Results. Figure 2 features the computed boundaries of RW and WFW. The use of a continuation method allows us to obtain continuous and complete boundaries of both workspaces, even in this situation with nonzero free length springs.

The RW is discontinuous, with two subspaces separated by unreachable configurations. Boundaries of the workspace arise from the different types of limits as featured on the left plot of Fig. 2. It shows the interest of the presented approach for the determination of the workspace. Note that internal force limits (outlined in black) correspond to configurations where $l_1 = l_0$ and tension in the spring AD is null. Then the mechanism is no longer preloaded.

The WFW is computed as the intersection of the enclosed spaces obtained for each sample in F_p. In Fig. 2, only the workspaces obtained for the minimum, maximum, and null value of F_p are represented. One can clearly observe the mechanism reconfiguration under an external load, and its impact on the workspace size. To our knowledge, this constitutes the first evaluation of the workspace that can be effectively reached by a tensegrity mechanism under external loads, with realistic nonzero free lengths. More precisely, one can first observe that for $F_p = F_{\max}$, the two separated subspaces of the RW can be joined (see the enclosed space by the red dotted lines). The impact of the external load is also modulated by the location in the workspace. In this example, the right part of the WFW is only 15% smaller than that of the RW, whereas the left part is reduced by 50%. This computational strategy allows observation of the nonintuitive behavior of a tensegrity mechanism.

4 Conclusions

In this paper, a definition for the workspace of tensegrity mechanisms was introduced. This definition is generic, taking into account physical limits of the components and the influence of the external load on the mechanism behavior.

A workspace estimation method was then proposed, that is based on a sampling of the external wrench and a computation of the corresponding RW by determining the boundaries introduced by each existing limit constraint. The considered continuation-based technique appears as efficient in the developed example. The application to a 2DOF planar tensegrity mechanism shows also the interest of the approach, with a WFW that constitutes meaningful information for the designer. Even on such a simple planar architecture, nontrivial results arise with discontinuous RW and WFW.

The workspace estimation can be refined, in particular by implementing an automatic detection of singular configuration. The method will also now be applied on other case studies in order to help in the design of novel spatial tensegrity mechanisms.

Acknowledgment

This work was supported by French state funds managed by the ANR within the Investissements d'Avenir programme (Labex CAMI—ANR-11-LABX-0004) and by the Région Alsace.

References

[1] Motro, R., 2003, *Tensegrity: Structural Systems for the Future*, Butterworth-Heinemann, London.
[2] Skelton, R. E., and Oliveira, M. C. D., 2009, *Tensegrity Systems*, Springer, New York.
[3] Arsenault, M., and Gosselin, C., 2006, "Kinematic, Static and Dynamic Analysis of a Planar 2-DOF Tensegrity Mechanism," Mech. Mach. Theory., **41**(9), pp. 1072–1089.
[4] Crane, C., Bayat, J., Vikas, V., and Roberts, R., 2008, "Kinematic Analysis of a Planar Tensegrity Mechanism With Pre-Stressed Springs," *Advances in Robot Kinematics: Analysis and Design*, J. Lenarcic and P. Wenger, eds., Springer, Dordrecht, pp. 419–427.
[5] Ji, Z., Li, T., and Lin, M., 2014, "Kinematics, Singularity, and Workspaces of a Planar 4-Bar Tensegrity Mechanism," J. Rob., **2014**, p. 967251.
[6] Koizumi, Y., Shibata, M., and Hirai, S., 2012, "Rolling Tensegrity Driven by Pneumatic Soft Actuators," IEEE International Conference on Robotics and Automation (ICRA), Saint Paul, MN, May 14–18, pp. 1988–1993.
[7] Aldrich, J., Skelton, R. E., and Kreutz-Delgado, K., 2003, "Control Synthesis for a Class of Light and Agile Robotic Tensegrity Structures," American Control Conference (ACC), Denver, CO, June 4–6, pp. 5245–5251.
[8] Tibert, A., and Pellegrino, S., 2003, "Review of Form-Finding Methods for Tensegrity Structures," Int. J. Space Struct., **18**(4), pp. 209–223.
[9] Mohr, C. A., and Arsenault, M., 2011, "Kinematic Analysis of a Translational 3-DOF Tensegrity Mechanism," Trans. Can. Soc. Mech. Eng., **35**(4), pp. 573–584.
[10] Ebert-Uphoff, I., and Voglewede, P., 2004, "On the Connections Between Cable-Driven Robots, Parallel Manipulators and Grasping," IEEE International Conference on Robotics and Automation (ICRA '04), New Orleans, LA, Apr. 26–May 1, pp. 4521–4526.
[11] Charpentier, I., 2012, "On Higher-Order Differentiation in Nonlinear Mechanics," Optim. Methods Software, **27**(2), pp. 221–232.
[12] Haug, E. J., Luh, C.-M., Adkins, F. A., and Wang, J.-Y., 1996, "Numerical Algorithms for Mapping Boundaries of Manipulator Workspaces," ASME J. Mech. Des., **118**(2), pp. 228–234.
[13] Seydel, R., 2010, *Practical Bifurcation and Stability Analysis*, Springer, New York.